Landslides (2023) 20:127–141
DOI 10.1007/s10346-022-01978-5
Received: 17 April 2022
Accepted: 13 October 2022
Published online: 12 November 2022

Changbao Guo · Yongshuang Zhang · Hao Yuan · Dingtao Liu · Yiqiu Yan · Shuai Hua · Sanshao Ren

Study of an ancient landslide reactivation mechanism based on centrifuge model testing: an example of the Jiangdingya ancient landslide reactivation in 2018, Gansu Province, China

Abstract The Jiangdingya (JDY) ancient landslide is a large-scale landslide located in the Bailongjiang River fault zone, Zhouqu County, Gansu Province. Affected by fault activities, rainfall, river erosion, and human engineering activities, the JDY landslide has been repeatedly reactivated and blocked the Bailongjiang River, causing great disasters. To study the reactivation mechanism of the JDY ancient landslide, based on field geological survey, the centrifuge simulation tests of the landslide body under 10%, 15%, and 20% water content conditions are carried out. The tests show that when the water content is 10%, only a few cracks are generated in the middle and rear parts of the slope by the end of the test, but the landslide is still in a stable state overall. However, when the water content is 15% and 20%, the landslide body is damaged, and the centrifugal acceleration required for slope instability is 100 g and 50 g, respectively. The test analysis shows that the JDY ancient landslide demonstrates composite retrogressive sliding. The deformation starts from the middle and rear parts of the slope, and cracks are generated. Then, the cracks gradually expand to the front edge. Under the river erosion influence of the slope toe, the cracks finally penetrate and cause landslide damage. The deformation process of the landslide body is mainly divided into four stages: ① consolidation; ② deformation initiation (crack formation stage); ③ deformation acceleration (crack acceleration development stage); and ④ instability. The centrifugal simulation tests suggest that the factors for JDY ancient landslide reactivation are mainly affected by rainfall and pore water pressure, as well as the coupling of sliding caused by the erosion of the river front with the movement of the middle and rear parts of the landslide caused by rainfall. At present, the JDY ancient landslide is still in a state of creeping deformation. It is necessary to pay close attention to the development of the cracks at the rear edge of the landslide and strengthen the prevention measures for landslide deformation instability and river blocking disasters.

Keywords Jiangdingya · Ancient landslide · Landslide starting · Centrifuge model test · Reactivation mechanism

Introduction

Due to the complex geological structural activity, topography and geomorphology, the Bailongjiang River Basin in Gansu Province is one of the most developed geological disaster areas both in China and in the world, and characterized by frequent occurrences and significant reactivations. Ancient landslides generally refer to landslides that have slipped since the Quaternary period and are the product of the long-term complex evolution of slopes (Cruden and Varnes 1996; Zhang et al. 2018). Ancient landslides are mostly stable but may be reactivated or slip again (Zhang et al. 2018). The reactivation of ancient landslides might be influenced by natural factors, such as precipitation, river erosion, and earthquakes, which might also be induced by human engineering activities (Yin et al. 2010; Deng et al. 2017). In recent years, ancient landslide reactivation disasters have occurred frequently and have caused tremendous losses, which have further attracted the attention of researchers to investigate ancient landslide deformation and hazards. For example, in the 1950s, the ancient landslide in Wolong Temple along the Xi'an-Baoji section of the Longhai Railway was reactivated, with a volume of approximately 2.0×10^7 m^3, and the Longhai Railway was pushed southward by more than 100 m (Li et al. 2013). In the mid-1990s, the ancient landslide at Badu Station of the Nanning-Kunming Railway was reactivated, and the treatment cost reached more than 90 million yuan (Li et al. 2013). In 2014, the Oso ancient landslide reactivated again in Washington State, USA, and the reactivated volume reached 760×10^4 m^3, which buried highway SR530 and caused 43 deaths (Iverson et al. 2015). Ancient landslide reactivation phenomena has been an important research topic and problem worldwide (Huang et al. 2011; Sassa and He 2013; Zhang et al. 2018).

On July 12, 2018, the Jiangdingya (JDY) ancient landslide was reactivated in Nanyu town, Zhouqu County, Gansu Province (Fig. 1a), and the newly occurred landslide volume was approximately $480–550 \times 10^4$ m^3. The landslide accumulation blocked the river channel, resulting in a half-dammed lake on the Bailongjiang River, which caused a water level rise, the interruption of the National Highway G345 (Fig. 1b), and the submersion of Nanyu village and Nanyu Power Station (Guo et al. 2020). Mu (2011) suggested that the JDY ancient landslide exhibits significant sliding characteristics with several different deeply buried sliding zones and sliding blocks and that the heavy rainfall, high-steep terrain of the landslide area, river erosion, and poor geotechnical properties are the main factors for landslide reactivation. Ma et al. (2020) deemed that the JDY landslide reactivation was mainly caused by rainfall based on InSAR detection results and rainfall data analysis and proposed that the landslide was formed by the coupling of internal and external dynamics. Although researchers currently believe that reactivation of the JDY ancient landslide was mainly induced by rainfall (Guo et al. 2020; Ma et al. 2020), there is still no

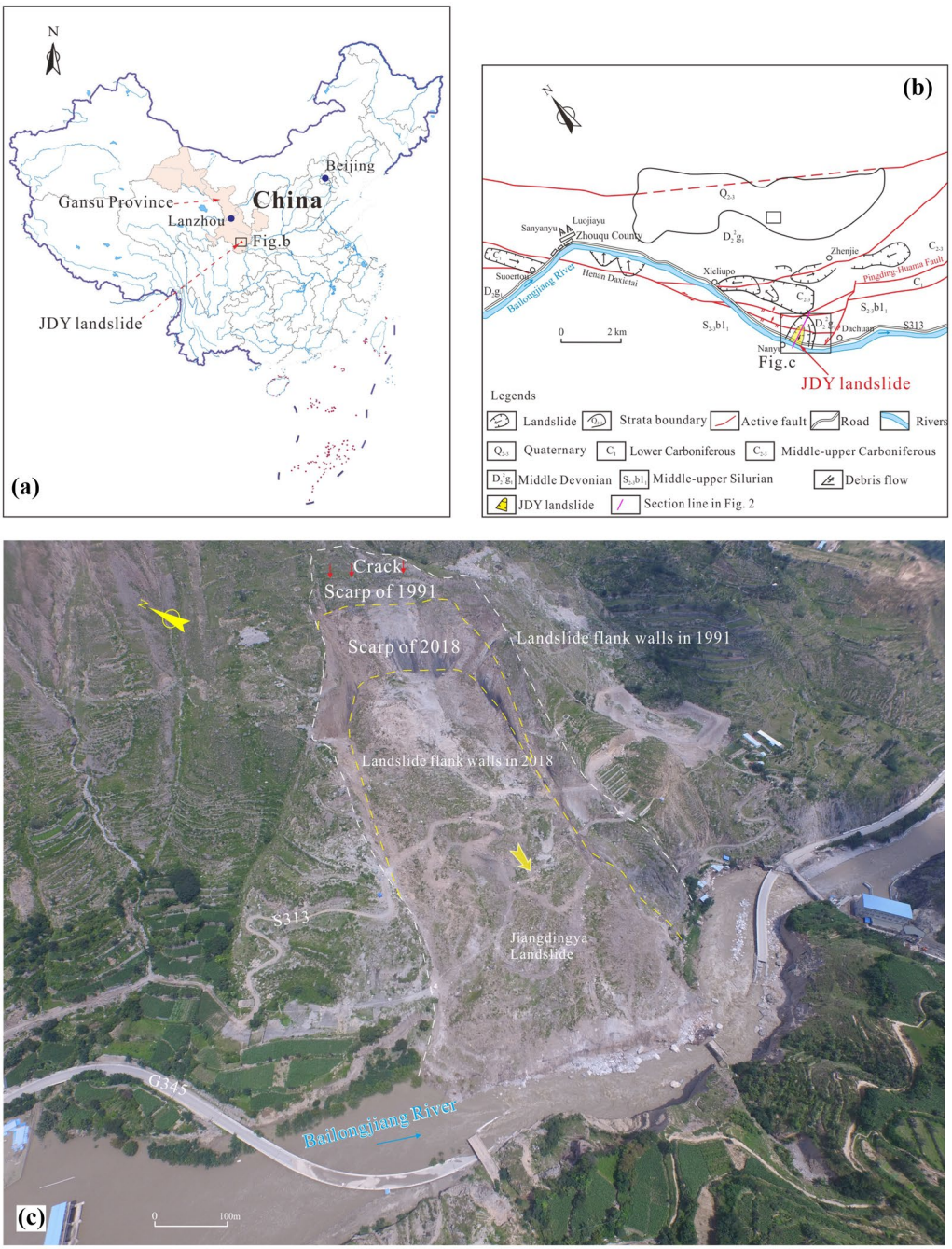

Fig. 1 The Jiangdingya landslide location and reactivation characteristics in 2018. **a** The location map of the study area; **b** the landslide distribution characteristics along the Bailongjiang River; **c** an overview of the reactivated JDY landslide in 2018 (photo by UAV)

clear understanding of the initiation mechanism of the JDY landslide. Furthermore, there are no relevant experimental or analysis results of the starting process and mechanism of JDY landslide reactivation, as no physical simulation test has been carried out, constraining disaster prevention and mitigation.

Many ancient landslide reactivation mechanism studies have been conducted by researchers worldwide. Physical modeling, engineering geological analysis, and numerical simulation are the main research methods (Zheng et al. 2022). Similar materials are used in the physical modeling method to reproduce slope deformation and failure processes, which can be achieved by simulating the changes in relevant factors in the slope evolution process and then analyzing its mechanical mechanism and deformation mechanism (Zhao et al. 2019; Wang and Zhang 2014). Physical modeling tests are the most intuitive methods for revealing landslide deformation and damage processes. Because ordinary laboratory small-scale model tests cannot simulate the in situ stress field and cause gravity distortion, the test results greatly deviate from actual observations;

however, the centrifuge test can make up for this deficiency (Boylan et al. 2010; Ng et al. 2016; Chan et al. 2018). The geotechnical centrifugal model test has unique advantages because it can reproduce a self-weight stress field and the deformation process related to the self-weight. The centrifugal model test has become a model test method for ancient landslide reactivation mechanics with good similarity to the prototype and has been widely used to reveal the mechanism of landslide disasters (Feng et al. 2013). During a centrifuge landslide modeling test, high pore water pressures can be measured and analyzed (Boylan et al. 2010; Chan et al. 2018), which is an important factor in landslide initiation analysis (Wang and Jiang 2017). Therefore, in this study, the JDY ancient landslide reactivation mechanism in 2018 was studied by centrifuge physical modeling tests. The development process of reactivation deformation of the JDY landslide under different water content conditions and the evolution trend of the displacement field in the landslide damage process were examined. The internal stress–strain response law and pore pressure growth mode revealed the mechanism of the JDY ancient landslide reactivation. The research results could help regional disaster prevention and mitigation and ancient landslide reactivation mechanism research.

Geological background

Regional geohazard development characteristics

The JDY ancient landslide, which is also named the Nanyu landslide (Wang et al. 1994; Mu 2011), is located at the foot of Tanyao Mountain and on the left bank of the Bailongjiang River in southeastern Zhouqu County (Fig. 1), Gansu Province, China. The geological structure around the JDY ancient landslide is very complex, with deep incised river valleys and high surface elevation relief, of which the elevation difference is up to 2300 m. The JDY ancient landslide is located in the Bailongjiang active fault zone, and the faults are mainly distributed in the NWW-EW direction, with strong activities in the Holocene and frequent historical earthquakes. For example, in 1879, a strong earthquake of Ms 8.0 occurred in the south of Wudu County to Wenxian County and caused many earthquake landslides. The average annual rainfall around the JDY landslide is approx. 433 mm/a, and the rainfall is mainly distributed form June to September and accounts for approx. 80% of the annual rainfall (Jin et al. 2022), and with many torrential rains. The maximum rainfall in the last 45 years is approx. 584.1 mm in 2019.

Due to the influence of active faults, historical strong earthquakes, rainfall, and human engineering activities in the study area, a series of serious geohazards occurred in recent years, of which the most devastating Sanyanyu debris flow occurred on August 8, 2010, after a heavy rainfall of 97 mm in 40 min in Zhouqu County, Gansu Province (Zhao et al. 2022), and the Xieliupo landslide experienced multiple reactivations and slidings (Jiang et al. 2016).

Engineering geology characteristics of the JDY landslide

Characteristics of the JDY ancient landslide

The JDY ancient landslide is distributed in a dustpan shape on the plane, and the rear wall of the landslide is generally in a chair shape (Fig. 3). The Pingding-Huama fault of the Bailongjiang fault zone passes through the middle and rear of the JDY ancient landslide. According to remote sensing interpretation and field geological survey, the JDY ancient landslide is approx. 2.02 km long and approx. 923 m in height difference between the top and bottom, and approx. 1500–1800 m in lateral width, with an area of 3.11 km^2, Guo et al. (2020) divided the JDY ancient landslide into three zones: the collapse zone, landslide rock mass deformation zone, and ancient landslide accumulation zone. The volume of the JDY ancient landslide accumulation zone volume is approx. $41 \sim 49 \times 10^6 m^3$, and there are obvious reactivation characteristics in the accumulation zone, where the staggered platform developed on it showed many reactivations.

The JDY ancient landslide has experienced more than 10 recorded reactivations since its first reactivation in 1807, including those in 1982, 1984, 1986, 1988, 1990, 1991, 2007, 2010, and 2018, among which the four large-scale reactivations in 1991, 2007, 2010, and 2018 dammed the Bailongjiang River (Wang et al. 1994; Mu 2011; Guo et al. 2020; Ma et al. 2020). On September 11, 1990, millions of cubic meters of the JDY ancient landslide body were reactivated, and the reactivated landslide pushed the road at the slope foot to the middle of the Bailongjiang River, dammed the Bailongjiang River and caused a cutoff for 8 h (Wang et al. 1994). On June 13, 1991, the JDY ancient landslide reactivated again. The reactivated landslide was 640-m long, 240-m wide and 30–40-m thick, and the landslide volume was approximately 6.4 million m^3, which dammed the Bailongjiang River and cut off flow for more than 9 h. The main factor causing the reactivation of the landslide was the 40-min torrential rain on June 8, which directly induced the occurrence of the landslide (Wang et al. 1994).

Reactivation characteristics of the JDY landslide on July 12, 2018

The volume of the JDY ancient landslide is approximately $640–970 \times 10^4$ m^3, with a total length of 640–700 m and a width of 240–250 m (Fig. 2). On July 12, 2018, the JDY ancient landslide reactivated again. The newly reactivated landslide was in the shape of a long tongue, with a length of approximately 580 m, a width of approximately 300 m at the front, 190 m at the middle, 185 m at the trailing edge, and an area of approximately 0.12 km^2. The occurrence of landslides is greatly affected by rainfall (Guo et al. 2020; Ma et al. 2020). A clear sliding shear zone and exposed bedrock can be seen on the sidewall of the sliding body (Fig. 2a). Based on drilling, a thick sliding zone composed of intensely broken limestone, slate, and carbonaceous phyllite was revealed (Fig. 2b), indicating that the average thickness of the sliding body is approximately 40–50 m, and the volume is $480–550 \times 10^4$ m^3. Guo et al. (2020) concluded that the water content of the JDY landslide sliding zone was 14.03% when it slipped, which is a typical landslide caused by heavy rainfall.

Engineering geomechanical properties of the sliding zone soils

The sliding zones were surveyed in the steep wall of the JDY landslide rear edge, the sidewall of the landslide, and the boreholes in the middle of the landslide, the depths of Zk1, ZK2, Zk3, and Zk4 were 47.7 m, 53.0 m, 61.6 m, and 54.2 m respectively (Figs. 2 and 3), and revealed the sliding zone depth of 19.0 m, 23.1 m, 27.2 m, and 25.5 m respectively. The sliding zones were characterized with dark gray, greenish gray contents, and clearly identifiable slip surface scrapes.

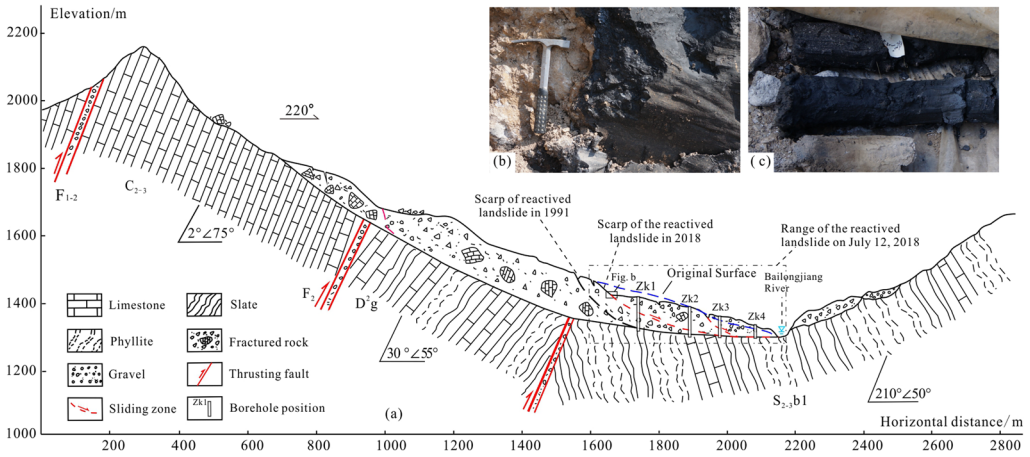

Fig. 2 **a** Engineering geological profile of the Jiangdingya ancient landslide; **b** the relationship between the sliding zone on the sidewall of the landslide and the exposed bedrock; **c** the characteristics of the sliding zone soil exposed by the Zk3 borehole

The tests show that the sliding zone moisture content is high, and the water content of the surface layer of the sliding zone at the trailing edge is 9.74%, the water content of the interior of the sliding zone at a position 0.5 m below the surface of the trailing edge is 20.76%, and the dry density is 2.01–2.03 g/cm^3. The water content of the sliding zone at the 29.8 m section of borehole Zk3 is approximately 14.03% (Fig. 2b), with a density of 2.16–2.25 g/cm^3, a cohesion c of 27.0 kPa, and an internal friction angle φ of approximately 30.5°. The borehole Zk3 is located at the middle and front parts of the sliding body, because there is a drainage phenomenon during the shearing process, so that the water content of the sliding zone soil at the middle and front parts of the JDY landslide body is lower than the water content of the sliding zone soils at the JDY landslide trailing edge. The subsurface water content at the JDY landslide back edge is closer to the water content of the JDY landslide initiation stage. According to the mechanical strength characteristics of different sliding zone soils of the JDY landslide, the high clay content and high density of the sliding zone soils indicated that the JDY landslide shear zone soils were compressed and compacted during sliding process, and resulting the shear strength of the sliding zone soils at the landslide leading edge is higher than that of general sliding zone soils. As a result, the JDY ancient landslide was characterized with slow sliding in 2018, other than fast and high-speed sliding.

Experimental methodology

Geotechnical centrifuge test principle

The geotechnical centrifuge model test scales the model to a certain scale, places it in a centrifuge, and then amplifies the centrifugal acceleration obtained by amplifying the acceleration of gravity at the same scale (Wang and Zhang 2014; Zhang, et al. 2017). Because of the high equivalence of the inertial force and gravity, which make the stress and strain of the model equal to that of the prototype, the deformation is similar between the centrifuge model and prototype, and the failure mechanisms of the centrifuge model and prototype are the same, so that according to the centrifuge model test results, we can reproduce the deformation and failure process of the prototype. The basic principle is that the scaled-down physical model is placed in a large-scale geotechnical centrifuge rotating

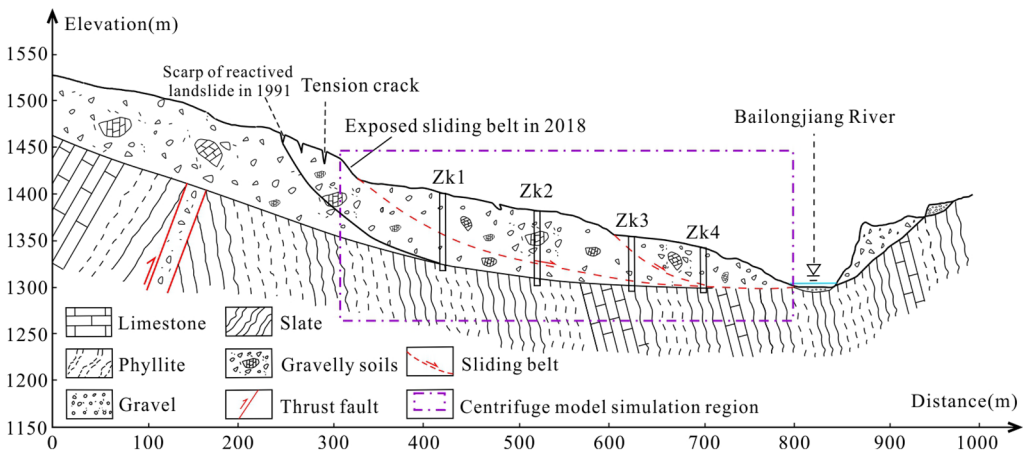

Fig. 3 Engineering geological profile of Jiangdingya ancient landslide reactivation and centrifuge physical modeling area

at high speed, and the model will be affected by high centrifugal acceleration during the test process. When the centrifugal acceleration is appropriate, the centrifugal force generated by the model is just right and can be used to compensate for the loss of self-gravity due to scaling down of geological models (Bowman et al. 2010).

Centrifuges were first used in geotechnical engineering research in 1973, and geotechnical centrifuges have been widely used in slope stability and landslide formation mechanism research (Boylan et al. 2010; Feng et al. 2013; Ng et al. 2016; Chan et al. 2018; Kennedy et al. 2021). For example, the centrifuge tests have revealed the topping deformation laws of landslides and some landslides formation mechanism under the influence of rainfall and gravity (Li et al. 2017; Zheng et al. 2022).

Centrifuge facility

The TLJ-500 geotechnical centrifugal testing machine was used in this test, which is composed of a centrifuge host, a 900 kW DC motor, a data acquisition and transmission system, a drag system, a monitoring system, a data processing system, a model box, and a manipulator. The maximum capacity is 500 g·t, and the maximum centrifugal acceleration can reach 250 g. The maximum size of the model box is 1.2 m (length) × 1.0 m (width) × 1.2 m (height) (Table 1).

Landslide physical model

Landslide prototype

Landslide physical modeling was used to inverse and analyze the JDY landslide reactivation and initiation mechanism in 2018, and the simulation range was mainly the reactivation zone in 2018 (Fig. 3).

Centrifuge model scale and structure

Prototype size, centrifuge capacity, model box size, nature of the research problem, and simulation accuracy should be considered comprehensively in model scale selection. According to the prototype of the JDY ancient landslide and the scope of the landslide area, the horizontal distance is close to 600 m, the maximum landslide width is 300 m (leading edge), and the landslide height is 180 m. The maximum size of the test model box is 1.2 m (length) × 1.0 m (width) × 1.2 m (height), and the similar material density and model quality could not meet the test requirements. Therefore, based on the comprehensively considered model size and prototype conditions, the design model size was selected as 1.0 m in length × 0.5 m in width × 0.3 m in height, and the model scale n was selected as 600. The similarity ratio of the main physical quantities between the centrifuge model and the landslide prototype is shown in Table 2. When preparing the model, the physical quantities of the model were designed in strict accordance with the corresponding similar proportions. According to the landslide prototype structure, the model structure mainly includes a sliding bed, a sliding body, and a sliding zone.

Table 1 Main parameters of the TLJ-500 geotechnical centrifuge

Technical parameters	Parameter value
Maximum capacity	500 g·t
Effective radius	4.5 m
Acceleration range	10–250 g
Effective load	Maximum 5 t under 100 g; Maximum 2 t under 250 g
Bucket volume	1.4 m × 1.5 m × 1.5 m
Model box	1.2 m × 1.0 m × 1.2 m, with a quality of 1.214 t

Test conditions

To reveal the development process of the reactivation and deformation of the JDY ancient landslide, the landslide body and sliding zone materials taken in the field were used for laboratory test remodeling. The moisture content of the prepared samples was close to that of the soil at the rear edge of the landslide, 0.5 m below the surface, and the sliding zone soil at the depth of the borehole; the water contents were 10%, 15%, and 20%, respectively. During the test, the loading centrifugal acceleration was gradually increased to simulate the landslide instability phenomenon. The test conditions are shown in Table 3. The test process was mainly divided into the consolidation stage and landslide deformation simulation stage.

Mechanical parameters of the model material

Sliding bed material

The sliding bed of the JDY landslide is mainly composed of carbonaceous slate, phyllite, and sandstone intercalated with limestone. Before constructing the centrifugal model, a similar material selection and ratio was first determined according to the three similarity theorems and the main scale relationship of the centrifugal model test (Zheng et al. 2022). The sliding bed was finally determined to be mixed according to a certain weight ratio of barite powder, crushed stone, quartz sand, gypsum, and water (Table 4).

Table 2 Similarity ratio of the centrifuge model and prototype

Variables	Model to prototype ratio	Variables	Model to prototype ratio
Acceleration	n:1	Cohesion	1:1
Length	1:n	Internal friction angle	1:1
Area	$1:n^2$	Poisson's ratio	1:1
Volume	$1:n^3$	Penetration coefficient	n:1
Water content	1:1	Time	$1:n^2$
Density	1:1	Porosity ratio	1:1
Bulk density	n:1	Stress	1:1

Table 3 Centrifuge model test plans

Number	Centrifuge acceleration loading stage	Water content
LST-1	(1) The acceleration is gradually increased from 0 to 50 g, and the model rotates at a constant speed for 5 min under the maintained 50 g acceleration (2) The acceleration is gradually increased from 50 to 150 g (2 min per 10 g) (3) The centrifuge model rotates at a constant speed for a certain period of time at a 150 g acceleration until slope failure or remains stable	10%
LST-2	(1) The acceleration is gradually increased from 0 to 50 g, and the centrifuge rotates at a constant speed for a certain period of time at the maintained 50 g acceleration (2) The acceleration is gradually increased from 50 to 100 g (2 min per 10 g) (3) The centrifuge model rotates at a constant speed for a certain period of time at a 100 g acceleration until the slope failure or remains stable	15%
LST-3	(1) The acceleration is gradually increased from 0 to 30 g, and the centrifuge rotates at a constant speed for 3 min under the maintained 30 g acceleration (2) The acceleration is gradually increased from 30 to 50 g (3) The centrifuge rotates at a constant speed for a certain period of time at the maintained 50 g acceleration until the slope failure or remains stable	20%

Sliding body, sliding zone material

To reflect the exact physical and mechanical properties of the prototype rock and soil mass of the landslide, the sliding body and the sliding zone in this test were made of the prototype materials taken from the landslide field site, and the particle size ratio adopted was determined according to the on-site material gradation. Minor adjustments and physical mechanical tests were performed on the proportioning materials so that the mechanical parameters of the sliding body and the sliding zone were close to those of the field site (Table 5).

Measurement systems

Monitoring instruments

There are seven TY1008 earth pressure sensors, three KY1008 pore water pressure sensors, and a multiangle camera were adopted in this centrifuge simulation test (Fig. 4), of which the monitoring instruments were specifically developed for the centrifuge by the General Engineering Research Institute, Chinese Academy of Engineering Physics.

Table 4 Proportioning table of similar materials for the sliding bed

Material name	Material percentage
Barite powder	40.9%
Quartz sand	27.2%
Gypsum	11.4%
Cement	9.1%
Water	11.4%

According to the "Pressure Sensor (Static) Verification Regulations (JJG 860–94)," the earth pressure and pore water pressure sensors were calibrated according to the factory inspection results of each sensor before being input into the model. For example, during the pore water pressure sensors verified, the digital multimeter HP 34401A was used, the current values of the pore pressure sensors were tested and recorded twice under different standard loads, such as 0 kPa, 200 kPa, 400 kPa, 600 kPa, 800 kPa, and 1000 kPa. According to the statistics and comparison with the factory value, the calibration results shew that the three pore water pressure sensors of KY-1, KY-2, and KY-3 fit well, and their nonlinearities were 0.05% FS, 0.04% FS, and 0.05% FS respectively, which meet the requirements of the centrifuge specification and the pore water pressure acquisition.

Monitoring instruments arrangement

All the monitoring instruments were connected to the control system by cables. The principles of the monitoring sensors layout are as follows:

Table 5 Values of the mechanical parameters of the sliding body and sliding zone

Water content	Material name	Model (cohesion c/kPa)	Model (angle of internal friction φ/°)
10%	Sliding body	32.3	35.1
	Sliding zone	29.5	20.6
15%	Sliding body	25.0	32.9
	Sliding zone	23.2	13.8
20%	Sliding body	20.1	25.2
	Sliding zone	17.0	7.7

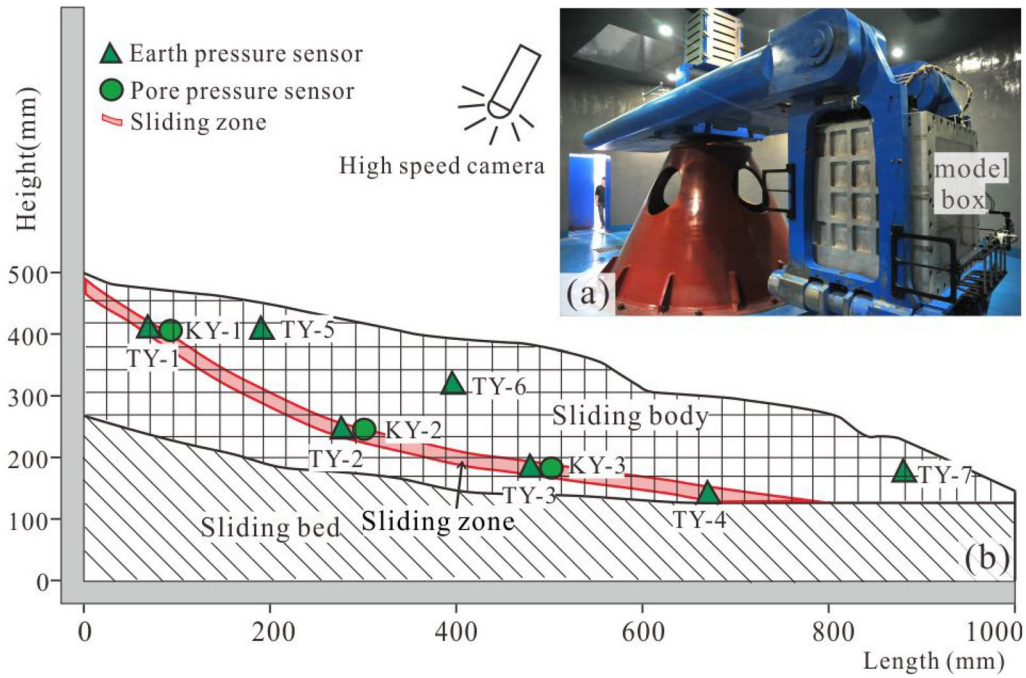

Fig. 4 **a** Photograph of the TLJ-500 centrifuge test equipment and **b** the sensors layout for the centrifuge modeling test

1. Arrangement of the 7 earth pressure sensors: The TY-1, TY-2, TY-3, and TY-4 earth pressure sensors were arranged in the sliding zone from top to bottom. There were 3 additional earth pressure sensors distributed at the trailing edge (TY-5), in the middle (TY-6), and at the leading edge (TY-7) of the sliding body. The measurement range of the earth pressure sensor was 1.0 MPa, with a diameter of 1.4 cm.
2. Arrangement of the 3 pore water pressure sensors: The three pore pressure sensors KY-1, KY-2, and KY-3 were arranged in the sliding zone from top to bottom, and the measurement range of the pore pressure sensor was 500 kPa, with a diameter of 1.4 cm. The positions of the TY sensor and the KY sensor were separated by 2 cm.
3. A multiangle camera: A real-time camera with 20 million pixels was fixed on the top of the model box and was used to capture the slope surface displacement and deformation of the landslide model.

Centrifuge model making process

The centrifuge model production process mainly included observation grid production (Fig. 5), sliding bed production, and sliding body and sliding zone (soft layer) production, and the produced model is shown in Fig. 5.

Analysis of the testing results

Deformation and failures of the JDY landslide

As shown in Fig. 6, in the LST-1 test period, when the water content of the sliding body was 10%, only a small number of cracks occurred in the middle and rear of the slope body after testing; the sliding body did not slide and was not destroyed during the whole test process.

Figure 7 shows that in the LST-2 test, when the water content was 15% and the centrifugal acceleration reached 40 g for 9 min, tensile cracks began to appear in the middle and rear of the slope body. When the centrifugal acceleration reached 50 g, the cracks gradually developed, and the cracks were generally arc-shaped, showing the nature of the pulling cracks. When the centrifugal acceleration increased from 60 to 100 g, the cracks gradually developed and penetrated the front edge, resulting in the overall sliding of the landslide.

From Fig. 8, in the LST-3 test, under the condition of a 20% water content, the cracks began to appear when the centrifugal acceleration was only 8 g for 3 min, and when the centrifugal acceleration increased to 9 g, the cracks developed rapidly. When the centrifugal acceleration was 13 g for 5 min, the cracks developed and penetrated to the front edge. When the soil at the front edge was squeezed by the soil from the rear section of the model, the soil body at the front edge experienced soil expansion. The acceleration continued to increase, and the slope continued to slide and fail (see Fig. 9).

Earth pressure variation analysis

1. When the water content was 10%, according to Fig. 10a, before the centrifugal acceleration was loaded to 150 g, the earth pressure gradually increased as the centrifuge acceleration increased, and the landslide mass and centrifugal acceleration were linearly correlated and jumped, indicating that the slope was in a stable state. The values of TY-5 and TY-7 increased

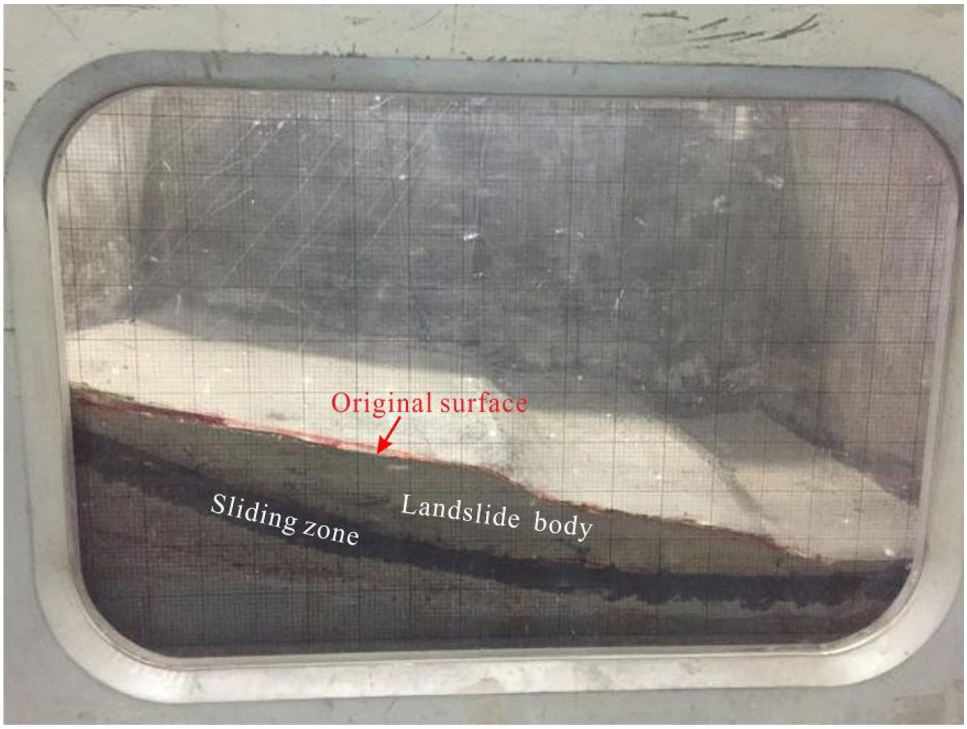

Fig. 5 Completed model of JDY landslide

slowly after the acceleration of the centrifuge was gradually loaded to 150 g, and the maximum values of TY-5 and TY-7 were 31.36 kPa and 34.77 kPa, respectively. The earth pressure indicated that the landslide body had been damaged in the middle, rear, and leading edges, and there was a trend of slight deformation. Figure 6a shows that there were some cracks in the landslide body at 9 min, but the whole slope body was still in a stable state.

2. When the specimen water content was 15%, according to Fig. 10b, the following results were determined: ① During the centrifugal acceleration period of 0–45 g, the earth pressure changing trend was consistent with the centrifugal acceleration changing trend. ② During the centrifugal acceleration period of 45–60 g, that is, the stage when the tension cracks began to occur on the slope body surface, the earth pressure of the TY-2 and TY-4 sensors suddenly dropped during the test, in the period from 9 to 11 min. The earth pressure drop was caused by crack occurrence and development in the slope at the same time (Fig. 7). ③ During the centrifugal acceleration stage of 60–100 g, slope cracks developed and expanded rapidly. From 9.8 to 18 min, the average growth rate of the earth pressure continued to increase, indicating that the centrifugal acceleration produced a slight increase, and the earth pressure increased rapidly. During this stage, the cracks in the slope developed rapidly in a very short period (Fig. 7d and e). ④ When the centrifugal acceleration was maintained at 100 g, the slope was in an unstable state. When the test progressed to 19 min, the TY-5 value suddenly dropped. At 20 min, the TY-6 value suddenly dropped, and the value of TY-6 fell behind that of TY-5. This phenomenon indicates that the deformation and

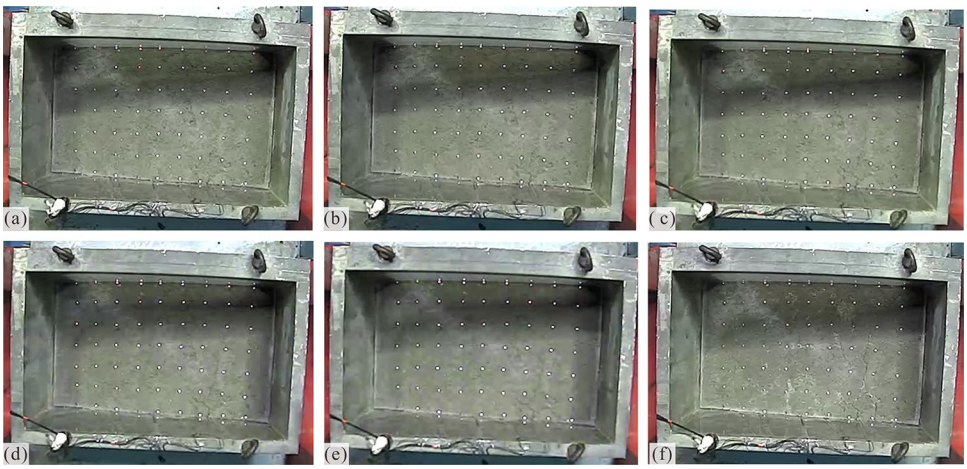

Fig. 6 The development process of cracks on the slope surface of the LST-1 test model when the water content is 10%. **a** The time is 9 min, and the acceleration is 50 g; **b** the time is 15 min, and the acceleration is 60 g; **c** the time is 16 min, and the acceleration is 80 g; **d** the time is 18 min, and the acceleration is 100 g; **e** the time is 19 min, and the acceleration is 120 g; **f** the time is 28 min, and the acceleration is 150 g

Fig. 7 The development process of cracks on the slope surface of the LST-2 test model when the water content is 15%. **a** The time is 7 min, and the acceleration is 30 g; **b** the time is 9 min, and the acceleration is 40 g; **c** the time is 10 min, and the acceleration is 50 g; **d** the time is 12 min, and the acceleration is 60 g; **e** the time is 14 min, and the acceleration is 80 g; **f** the time is 19 min, and the acceleration is 100 g

failure of the landslide started from the middle and rear edges and gradually developed to the front edge of the landslide. The slope had reached an unstable state. The experimental results show that JDY ancient landslide deformation is a failure mode of sliding landslides.

3. When the water content was 20%, according to Fig. 10c, the following results can be determined: ① During centrifugal acceleration from 10 to 30 g, the cracks were in the development stage. The increasing trends of TY-3 and TY-4 were basically the same. When the test was carried out for 10 min, the increasing trend of TY-3 and TY-4 was gradually larger than that of TY-2. With a gradual increase in centrifugal acceleration, the increasing trend of the TY-3 and TY-4 values was more obvious. This phenomenon shows that the cracks started from the middle and rear edges, and the thrust power at the landslide rear continuously increased and was continuously transmitted to the front edge of the landslide, resulting in a clearer increase in the earth pressure at the front edge of the landslide. ② At the centrifugal acceleration of the 30–50 g stage, the slope was in an unstable state. With increasing centrifugal acceleration, the thrust pressure at the landslide rear section part increased continuously to the landslide leading edge, resulting in the continuous expansion of cracks to the leading edge, and a landslide occurred finally.

Pore water pressure variation analysis

A total of 3 pore water pressure gauges, KY-1, KY-2, and KY-3, were arranged in this test (Fig. 4b).

1. According to Fig. 10a, under the condition of a 10% water content, the KY-1 value shows a negative growth, and the maximum pore water pressure is − 4 kPa, which indicates that the landslide body was unsaturated soil, and the water body penetrated the soil body mainly along the particles. Because there is a water–air meniscus between the soil particles (Egeli and Pulat 2011), the measured pore water pressure was negative, and the KY-3 value was larger than that of KY-2 during this period. When the test was carried out for 27 min, the KY-2 value suddenly increased to a maximum of 11.74 kPa, while the KY-3 value lag behind that of KY-2. At 32 min, the KY-3 value suddenly increased, with a maximum increase of 10.55 kPa. The pore water pressure values of KY-2 and KY3 suddenly increased because the landslide body squeezed forward during the test, and tension cracks began to appear in the middle and rear edges, from which the water flowed to the front edge in the sliding body. It can be seen from the earth pressure change trend diagram of Fig. 10a that TY-5 was the first to undergo deformation and failure, which led to the accumula-

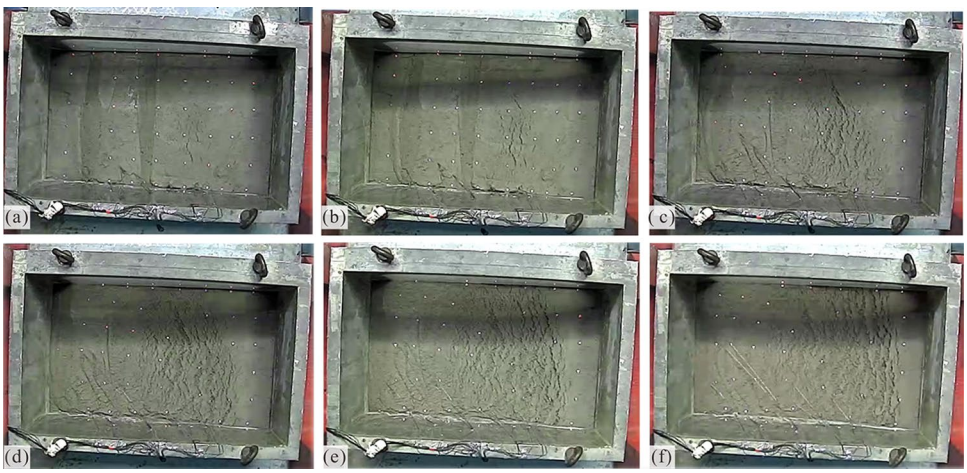

Fig. 8 The development process of cracks on the slope surface of the LST-3 test model when the water content is 20%. **a** The time is 3 min, and the acceleration is 8 g; **b** the time is 4 min, and the acceleration is 9 g; **c** the time is 5 min, and the acceleration is 13 g; **d** the time is 6 min, and the acceleration is 20 g; **e** the time is 7 min, and the acceleration is 30 g; **f** the time is 12 min, and the acceleration is 50 g

Fig. 9 Side view of the landslide state at the end of the centrifuge simulation test under different water content conditions. **a** Landslide failure form when the water content is 10%; **b** landslide failure form when the water content is 15%; **c** landslide failure form when the water content is 20%

tion of pore water at position KY-3, resulting in an increase in the KY-3 value. During the period when the acceleration was maintained at 140 g, the pore water pressure first remained unchanged and then suddenly increased, indicating that the landslide mass was displaced, deformed, and squeezed during this process, and the pore water pressure gradually increased.

2. According to Fig. 11b, under the condition of a 15% water content, the KY-2 value increased proportionally with the acceleration, and the KY-2 value was significantly larger than that of KY-1, which indicates that the landslide mass produces forward extrusion deformation failure during the test. When the test was in the 60–100 g stage, the KY-1 value decreased slowly from 19.53 to 15.66 kPa. When the acceleration was maintained at 100 g, the KY-2 value gradually increased, and a maximum of 138.21 kPa was attained. According to the earth pressure variation trend (Fig. 10b) and the landslide crack development process (Fig. 8), cracks began to occur in the middle and rear of the slope. The KY-1 value increased mainly because the water converges toward the front edge of the slope along the cracks in the middle and rear of the landslide body.
3. According to Fig. 11c, under the condition of a 20% water content, when the acceleration increased to 8 g, the KY-2 value was greater than that of KY-1. The development map of cracks on the slope surface in Fig. 10a shows that cracks started to develop in the middle and rear of the slope, and the rear soil was pressed forward, causing the KY-2 value to be greater than that of KY-1.

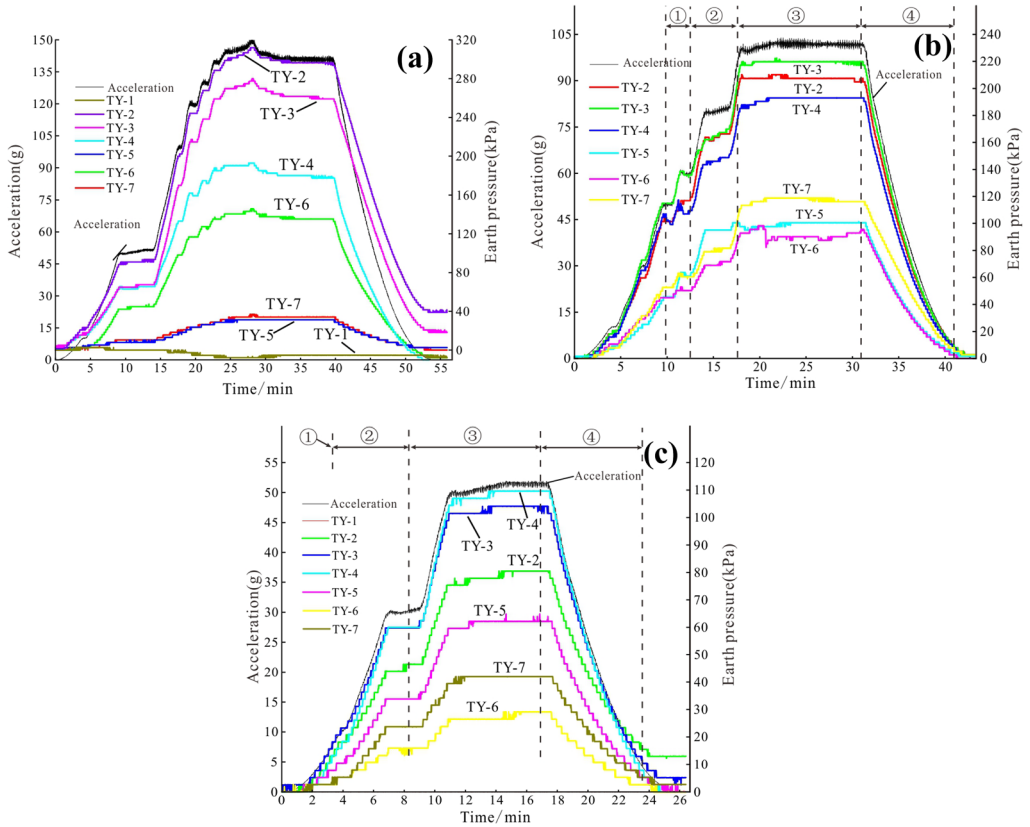

Fig. 10 The variation trend of earth pressure with acceleration under different water contents: **a** water content of 10%; **b** water content of 15%; **c** water content of 20%. ① Consolidation stage; ② deformation initiation stage; ③ deformation acceleration stage; ④ instability stage

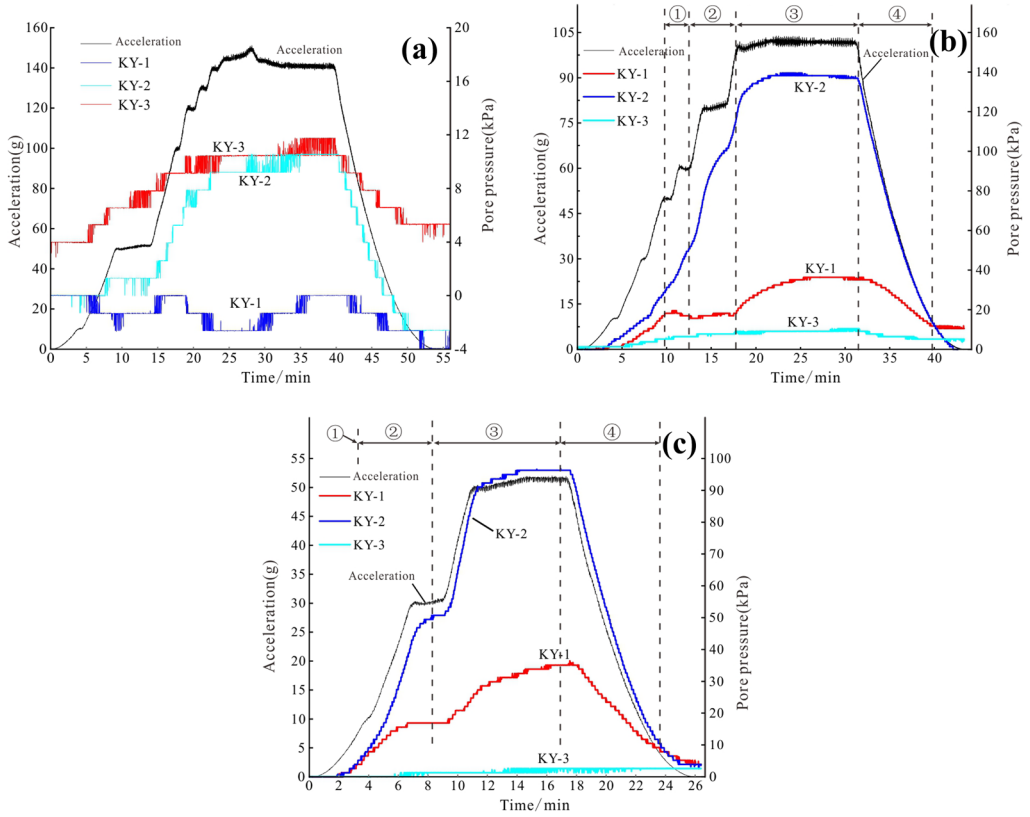

Fig. 11 The variation trend of pore pressure with acceleration under different water contents: **a** water content of 10%; **b** water content of 15%; **c** water content of 20%. ① Consolidation stage; ② deformation initiation stage; ③ deformation acceleration stage; ④ instability stage

When the acceleration reached 50 g and the test was carried out for 15 min, the KY-2 value reached a maximum value of 96.35 kPa. Meanwhile, the slope began to be unstable. During the period when the acceleration was maintained at 50 g, the growth rate of KY-1 and KY-2 was slow until it was flat, which indicates that under the action of a small centrifugal load, the sliding body produced displacement, deformation, and extrusion, and the slope body was in an unstable state, resulting in significant changes in the pore water pressure value.

Discussion

Analysis of the reactivation and initiation of the JDY ancient landslide

Variation analysis of the mechanical strength of the sliding zone soils

Previous studies have shown that landslide occurrences are mainly caused by a weakening of the mechanical strength of the sliding zone soil. To analyze the changing characteristics of the mechanical strength of the sliding zone soil, direct shear tests were carried out on sliding zone soil before and after landslide sliding at an LST-3 test water content of 20%. The test results show that the soil cohesion c is 17 kPa before the landslide occurrence and 12 kPa after the landslide; that is, there is a 5 kPa or 29.41% reduction in the sliding zone cohesion c due to sliding. The internal friction angle φ is 7.76° before the landslide occurrence and 5.58° after the landslide; that is, there is a 2.18° or 28.09% reduction in the internal friction angle φ due to sliding. When the water content of the landslide model is 20%, the deformation of the landslide greatly weakens the mechanical parameters of the sliding zone soil and induces a landslide occurrence.

Analysis of the landslide deformation process

Ma et al. (2020) deemed that rainfall is the main inducing factor of the JDY landslide reactivation, and they found that the precipitation was concentrated at 30–39 h before the landslide by the InSAR detection results and rainfall value. Infiltrating rain increases the water content (Ma et al. 2020) and pore pressure of the landslide (Wang and Jiang 2017). The landslide centrifuge physics simulation test indicates that the JDY landslide deformation is mainly controlled by the water content, and the deformation and failure gradually develop from the middle and rear of the slope. When the water content is 15%, the centrifugal acceleration at the beginning of cracks is 40 g, and the centrifugal acceleration at the time of instability is 100 g. However, when the water content is 20%, the centrifugal acceleration at the crack beginning is 8 g. The instability occurs when the centrifugal acceleration reaches 50 g.

According to the test, the deformation process of the landslide can be divided into the following three stages: (1) the deformation initiation stage, in which the cracks in the middle and rear of the slope begin to appear; (2) the deformation acceleration stage, in which the

middle and rear cracks develop and expand rapidly to the front edge of the slope; and (3) the instability stage, in which the tensile cracks expand and penetrate on the slope surface, a potential sliding zone is formed, and a landslide occurs.

The effect of rainfall on the reactivation of ancient landslides

Rainfall is one of the main factors that induce large-scale landslides. Lumb (1962) found that when the rainfall exceeded 100 mm within 24 h or the rainfall exceeded 350 mm within the previous 15 days, landslides were more likely to be induced. Ren et al. (2013) believed that when rainfall reaches 30 mm in Zhouqu County, Gansu Province, large-scale landslides can be easily induced. The accumulated rainfall in the JDY area within 15 days, from June 25 to July 10, exceeded 300 mm. Guo et al. (2020) believed that the rainfall reached a heavy rainfall level of 65 mm on July 10, and the relatively concentrated rainfall eventually led to the overall instability of the JDY landslide. Because the structure of the JDY landslide is loose and there are many cracks, it is easy for heavy rainfall to pass through the cracks to form infiltration channels. The rainfall infiltrates the sliding zone, which increases the water content

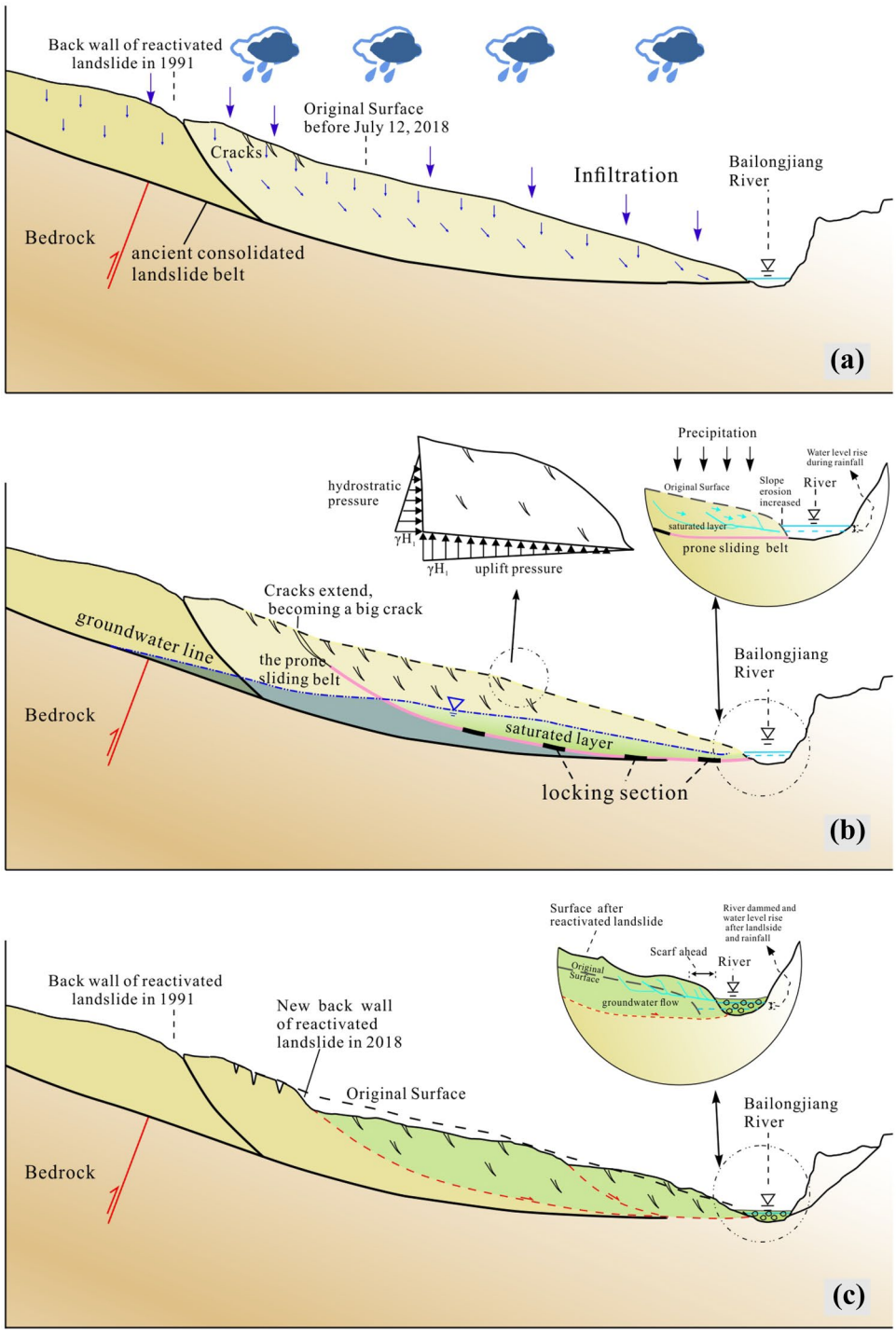

Fig. 12 The reactivation process model of the JDY ancient landslide on July 18, 2018. **a** The process of rainfall infiltration into ancient landslide bodies; **b** rainfall infiltration and river incision mechanism for landslide reactivation; **c** the newly reactivated landslide and dammed river lake

and softens the mechanics of the sliding zone soils. At the same time, the infiltrated rainfall forms the upper layer of stagnant water in the relative aquifer (carbonaceous slate), which increases the weight of the rock and soil mass, resulting in an increase in the sliding force and finally leading to the occurrence of the JDY landslide.

Influence of excess pore water pressure on landslide initiation during landslide deformation

The critical pore pressure for landslide initiation is mainly controlled by the density, the effective porosity of the slope rock and soil, the thickness of the overlying rock and soil on the potential slip surface, the cohesion and internal friction angle of the slope components, and the slope angle (Skempton and Delory 1957).

$$U\mathrm{wc} = \rho g z\left(1 - \frac{\tan\theta}{\tan\varphi}\right) + \frac{c}{\tan\varphi} \quad (1)$$

In Eq. 1, the θ is the inclination angle (°) of an inclined weak surface on the landslide, ρ is the density of the rock and soil mass (g/cm^3), g is the acceleration of gravity, z is the depth of the potential slip surface (m), c is the cohesion of the rock mass and soil mass (kPa), and φ is the internal friction angle of the rock mass and soil mass (°). According to Eq. 1, the critical pore pressure $U_{wc} = 67.27$ kPa can be obtained by taking θ = 30°, ρ = 2.16 g/cm^3, $g = 9.8$ m/s^2, $z = 0.3$ m, $c = 27$ kPa, and φ = 30.5°. When the water content of the slip body is 10%, the maximum pore water pressure is 11.77 kPa, which is less than the critical pore water pressure. However, the maximum pore water pressure in the test is 138.21 kPa and 96.35 kPa in the cases of 15% and 20%, respectively, which are both higher than the critical pore water pressure and eventually cause landslide slip.

The JDY ancient landslide reactivation mechanism

The reactivation mechanism of the JDY ancient landslide is very complex. The fractured rock and soil and the structural characteristics of the slope formed under the action of a fault and an earthquake provide the internal triggers of landslide reactivation. Heavy rainfall increases the weight of the slope and weakens the mechanical strength of the rock and soil. In particular, the strong river erosion formed during the rainstorm period further cut the slope toe, thereby inducing landslide reactivation, which is a typical retrogressive landslide (Guo et al. 2020), and ancient landslide reactivation may occur under the coupling of internal and external dynamic geological conditions (Guo et al. 2020; Ma et al. 2020).

According to the centrifuge physical modeling test results, combined with the field investigation, this study suggests that rainfall caused the water content to increase in the middle and rear parts of the JDY ancient landslide (Fig. 12) and that tension cracks initiated in the middle and rear parts, which subsequently induced the pushing effect. Under the river erosion and traction effect, a new composite retrogressive landslide reactivation model of the JDY ancient landslide was formed. That is, the coupled initiation mechanism of the river erosion and traction effect from the landslide front and the pushing effect from the middle and rear parts of the landslide eventually led to the reactivation of the JDY ancient landslide.

Centrifuge model tests have played an increasingly important role in landslide formation mechanism studies. In this study, the JDY ancient landslide reactivation process was analyzed by traditional monitoring sensors in centrifuge tests, such as earth pressure and pore water pressure sensors, and positive study results were obtained. In recent years, centrifuge tests have been used in complex landslide simulation analyses with new monitoring technology methods, such as fiber Bragg grating (FBG) sensing technology (Li et al. 2017; Zhang, et al. 2017), particle image velocimetry (PIV) (Weng et al. 2017), and point laser sensors (Archer and Ng 2018). The study results indicate that the centrifuge test combined with new monitoring sensors can obtain more precise displacement and deformation of the sliding body, as well as the soil pressure change of the landslide body before and after sliding. Therefore, the FBG, PIV, and point laser sensor are suggested to be used in future landslide centrifuge test studies to acquire and study the landslide deformation process.

Conclusions

In this paper, the reactivated JDY ancient landslide was taken as the main study prototype. Based on field investigations and sliding zone soil mechanics tests, the centrifuge model tests were carried out to study for the JDY landslide reactivation process, and the following conclusions and understandings were obtained.

First, rainfall is the main influencing factor for ancient landslide reactivation. The rainfall causes the soil water content to change, which reduces the soil strength to a certain extent. Rainfall causes changes in pore water pressure in the soil, which reduces the anti-sliding force of the soil. Therefore, the stability of the slope is reduced, which further leads to landslides.

Second, according to the slip-initiating process simulation of the landslide with different water contents, the variation law of soil pressure and pore water pressure was obtained when the landslide failed. The test also shows that the deformation and failure of the JDY ancient landslide develop gradually from the slope middle and rear. The smaller the centrifugal acceleration is, the larger the water content required for the landslide to start. When the water content is 15% and 20%, the centrifugal acceleration required for the slope stability to be lost is 100 g and 50 g, respectively. When the water content is 10%, only a small number of cracks occur in the middle and rear of the slope by the end of the test, which is consistent with the actual situation.

Third, the centrifuge model test shows that the JDY ancient landslide deformation process is mainly divided into three stages: the deformation initiation stage, when the cracks begin to form; the deformation acceleration stage, when the cracks develop rapidly; and the starting or instability stage.

Fourth, the heavy rainfall is the direct precipitating factor for JDY ancient landslide reactivation. Heavy rainfall infiltration leads to a decrease in the strength properties of the sliding zone soils. Coupled with the river erosion at the leading edge, a new composite retrogressive reactivation mechanism model is formed, which is characterized by the river erosion and traction effect from the landslide front part and the pushing effect from the landslide middle and rear parts.

Acknowledgements

The centrifuge model test was carried out in the State Key Laboratory of Geological Hazard Prevention and Geological Environmental Protection, Chengdu University of Technology, China. The authors would like to thank Associate Prof. Yang Ren, Associate Prof. Guang Zheng for their help in the test and Associate Prof. Zhihua Yang, Associate Prof. Xue Li, the postgraduate students, Jijun Jin and Jian Liu, from the Institute of Geomechanics, CAGS, who participated in the field work and data analysis.

Funding

This study was supported by the National Natural Science Foundation of China (no. 41877279, 41731287, and 41941017), the Outstanding Young Scientific and Technological Talent Project of the Ministry of Natural Resources (no. 12110600000018003911), and the China Geological Survey (no. DD20190319, 20190505).

Declarations

Conflict of interest The authors declare no competing interests.

References

Archer A, Ng CWW (2018) A new environmental chamber for the HKUST centrifuge facility. In Physical Modelling in Geotechnics, CRC Press, 489–493

Bowman ET, Laue JIB, Springman SM (2010) Experimental modelling of debris flow behaviour using a geotechnical centrifuge. Can Geotech J 47(7):742–762

Boylan N, Gaudin C, White DJ et al (2010) Modelling of submarine slides in the geotechnical centrifuge. In: Proceedings of the 7th international conference Physical Modelling in Geotechnics, Zurich, 1095–1100

Chan K, Zhang LM, Zhu H et al (2018) Centrifuge modelling of slope instability due to leakage of buried pipes: proceedings of China-Europe conference on geotechnical engineering. Springer Series in Geomechanics and Geoengineering 2:1453–1457

Cruden DM, Varnes DJ (1996) Landslide types and processes, special report, transportation research board. National Academy of Sciences 247:36–75

Deng H, Wu LZ, Huang RQ et al (2017) Formation of the Siwanli ancient landslide in the Dadu River. China Landslides 14(1):385–394

Egeli I, Pulat HF (2011) Mechanism and modelling of shallow soil slope stability during high intensity and short duration rainfall. Scientia Iranica 18(6):1179–1187

Feng Z, Yin YP, Li B et al (2013) Physical modeling of landslide mechanism in oblique thick-bedded rock slope: a case study. Acta Geologica Sinica (english Edition) 87(04):1129–1136

Guo CB, Zhang YS, Li X et al (2020) Reactivation of giant Jiangdingya ancient landslide in Zhouqu County, Gansu Province. China Landslides 17(1):179–190

Huang RQ, Wang YS, Wang ST et al (2011) High geo-stress distribution and high geo-stress concentration area models for eastern margin of Qinghai-Tibet plateau. SCIENCE CHINA Technol Sci 54(s1):154–166

Iverson RM, George DL, Allstadt K et al (2015) Landslide mobility and hazards: implications of the 2014 Oso disaster. Earth Planet Sci Lett 412:197–208

Jin JC, Chen G, Meng XM et al (2022) Prediction of river damming susceptibility by landslides based on a logistic regression model and InSAR techniques: a case study of the Bailong River Basin. China Engineering Geology 299:106562

Jiang S, Wen BP, Zhao C et al (2016) Kinematics of a giant slow-moving landslide in Northwest China: constraints from high resolution remote sensing imagery and GPS monitoring. J Asian Earth Sci 123:34–46

Kennedy R, Take WA, Siemens G (2021) Geotechnical centrifuge modelling of retrogressive sensitive clay landslides. Can Geotech J 58(10):1452–1465

Li LQ, Ju NP, Guo YX (2017) Effectiveness of fiber Bragg grating monitoring in the centrifugal model test of soil slope under rainfall conditions. J Mt Sci 14:936–947

Li TL, Wang CY, Li P (2013) Loess deposit and loess landslides on the Chinese Loess Plateau. Progress of geo-disaster mitigation technology in Asia. Springer, Berlin, Heidelberg, pp 235–261

Lumb (1962) Effects of rain storms on slope stability [C]// Proceedings, Symposium on Hong Kong Soils, Hong Kong Soils, Hong Kong, pp: 73–89

Ma SY, Qiu HJ, Hu S et al (2020) Characteristics and geomorphology change detection analysis of the Jiangdingya landslide on July 12, 2018, China. Landslides 18:383–396

Mu P (2011) Analysis on causes and stability of landslide at Jiangdingya in Zhouqu County of Gansu Province. China Water Resources 4:50–52 (in Chinese with English abstract)

Ng CWW, Song DR, Choi CE et al (2016) A novel flexible barrier for landslide impact in centrifuge. Géotechnique Letters 6(3):221–225

Ren D, Leslie L, Lynch M et al (2013) Why was the august 2010 Zhouqu landslide so powerful. Geography, Environmental, Sustainability 6(1):67–79

Sassa K, He B (2013) Dynamics and prediction of earthquake and rainfall-induced rapid landslides and submarine megaslides. Landslides: Global Risk Preparedness, pp: 191–211

Skempton AW, Delory FA (1957) Stability of natural slopes in London clay. Proc. 4th Int. Conf. on Soil Mech Found Eng 2:378–381

Wang G, Jiang Y (2017) High mobility of large-scale shallow landslide triggered by heavy rainfall in Izu Oshima. In: Mikoš, M., Casagli, N., Yin, Y., Sassa, K. (eds) Advancing Culture of Living with Landslides, 213–220. WLF 2017. Springer, Cham

Wang JR, Qi L, Cai XX (1994) Analysis on landslide of Nanyu in Zhouqu County of Gansu Province. Bull Soil Water Conserv 14(1):57–60 (in Chinese with English abstract)

Wang LP, Zhang G (2014) Centrifuge model test study on pile reinforcement behavior of cohesive soil slopes under earthquake conditions. Landslides 11:213–223

Weng MC, Chen TC, Tsai SJ (2017) Modeling scale effects on consequent slope deformation by centrifuge model tests and the discrete element method. Landslides 14(3):981–993

Yin YP, Zheng WM, Liu YP et al (2010) Integration of GPS with InSAR to monitoring of the Jiaju landslide in Sichuan. China Landslides 7(3):359–365

Zhang D, Xu Q, Bezuijen A et al (2017) Internal deformation monitoring for centrifuge slope model with embedded FBG arrays. Landslides 14:407–417

Zhang YS, Wu RA, Guo CB et al (2018) Research progress and prospect on reactivation of ancient landslides. Adv Earth Sci 33(7):728–740 (in Chinese with English abstract)

Zhao JJ, Xie ML, Yu JL et al (2019) Experimental study on deformation and failure mechanism of fill embankment slope due to engineering load. J Eng Geol 27(2):426–436 (in Chinese with English abstract)

Zhao Y, Meng XM, Qi TJ et al (2022) AI-based rainfall prediction model for debris flows. Eng Geol 296:106456

Zheng D, Zhou HK, Zhou H et al (2022) Effects of slope angle on toppling deformation of anti-dip layered rock slopes: a centrifuge study. Appl Sci 12(10):5084

Changbao Guo (✉) · Hao Yuan · Dingtao Liu · Yiqiu Yan
Institute of Geomechanics, Chinese Academy of Geological Sciences, Beijing 100081, China
Email: guochangbao@cags.ac.cn

Changbao Guo
Key Laboratory of Active Tectonics and Geological Safety, Ministry of Natural Resources, Beijing 100081, China

Yongshuang Zhang · Sanshao Ren
Institute of Hydrogeology and Environmental Geology, Chinese Academy of Geosciences, Shijiazhuang 050061, Hebei, China

Shuai Hua
North China Institute of Science and Technology, Langfang 065201, Hebei, China